Preparation and characterization of mechanically alloyed, yttria containing steel powder for additive manufacturing of dispersion strengthened steels

Semester project – A. Cavaliere

Subject:

Oxide-dispersion-strengthened (ODS) steel is a material that is being studied for its potential in high-temperature and high-irradiation applications, such as nuclear fusion reactors or generation IV fission reactors. Its properties derive from the presence of nano-dispersed oxide particles that act as a barrier against the movement of dislocations, hence reducing susceptibility to creep, and as sinks for irradiation-induced defects. In this study, a powder for additive manufacturing is produced with mechanical alloying (MA) in a planetary ball mill; seven sets of powders are produced in this study, each with a different set of milling parameters, so that the best-suited specimen for the chosen manufacturing process may be selected. The powder is studied with a Scanning Electron Microscope (SEM) imaging and optical microscopy in order to characterize the formation of the oxides with an acceptable level of detail and to determine the size distribution of the powder particles. The results show the choice of acetic acid and ethanol as process control agents for dry grinding of the powders does not improve the characteristics of the end product to a significant extent. An increase in the grinding time seems more effective in increasing the yield and reducing the average size of the particles to an acceptable range, but it may result in a compromise in terms of the powder's flowability.

Author: CN46	Signature:	Date: 7/02/2019	Reviewer: WP46	Signature:	Date: 7/02/2019

Distributor	Dep.	Addresses	Cop.	Dep.	Addresses	Cop.		Cop.
	4600	M.A. Pouchon	1*				Library	
	4600	TM-Dossier (Sekretariat)	1*				Total (print)	
	4601	P. Warnicke	1*				Pages	20
	4100	H.M. Prasser	1*				Attachments	
							Signature Head of Lab.:	

VOLNM07e Rev. 1

Version Updates

Revision	Date	Modification
Composed	18.01.2019	

Contents

1　　Introduction

The harsh conditions of nuclear fusion reactors and IV generation fission reactors exercise a variety of stresses on the materials employed. Besides the mechanical stresses caused by pressure gradients, thermal and irradiation-induced stresses are also a significant challenge that needs to be adequately answered; on top of this, high-cycle and low-cycle fatigue also limit the lifetime of the chosen materials. In this context, there is a strong interest in oxide-dispersion-strengthened (ODS) steels as good candidates because of their enhanced irradiation damage and thermal creep resistances [1]. In terms of mechanical properties the presence of the oxide particles typically results in increased yield stress and hardness but reduced ductility [2].

The formation of the oxide particles is clearly strongly affecting the material's properties and as such it is worth exploring in detail. In this study, powder samples with the targeted composition are produced through mechanical alloying of the metal and oxide powders (see composition in Table 1) via ball milling; the influence of the processing conditions on the properties of the powders is analyzed. The most suitable of these samples is to be used in Additive Manufacturing (AM) to produce an ODS steel specimen for further analyses and testing.　There is a growing interest in using additive manufacturing to attempt to produce ODS steel [3]; this method bears several advantages, such as freedom of design and and a decrease of assembling complexity [4]. However, in order to conduct a successful AM step, the feed powder should fulfil narrow specifications. Especially the flowability is of high importance for the successful handling of the powder in an automated process.

2　Production of samples

The samples have all been produced with mechanical alloying via ball milling, but with different parameters. The starting materials were:

- Eurofer-97 powder, with particles smaller than 150 μm;

- Yttrium oxide powder, 99.9% purity.

The exact composition of the powders can be read in table 1.

Table 1: Composition (in mass percentage) and weight fraction of the initial powders.

99.5% Eurofer	Fe	Cr	W	Mn	Y
	89%	9%	1.1%	0.4%	0.4%
	Ta	C	V	O	
	0.12%	0.11%	0.1%	0.1%	
0.5% Yttria	Y_2O_3	Dy_2O_3	Tb_4O_7		
	99.9%	0.1%	Traces		

Six samples were produced via dry grinding and one via wet grinding. The process parameters are summarized in table 2. All the samples but the wet milled one were milled in an inert Argon atmosphere, in order to prevent oxidation of the fine particles produced.

Table 2: Process parameters of the milled samples.

ID	Time	Mill	Pause	PCA	RPM	Mass	Jar fill	Ball
PA-2060	20h	10	15	Acetic acid	600	200 g	67%	5 mm
PA-4060	40h	10	15	Acetic acid	600	200 g	67%	5 mm
WE-0855[1]	8h	10	15	Ethanol	550	200 g	80%	2.5 mm
PE-2060	20h	10	15	Ethanol	600	200 g	67%	5 mm
PA-2045	20h	10	15	Acetic acid	450	200 g	67%	5 mm
D-2060	20h	10	15	//	600	200 g	67%	5 mm
D-4060	40h	10	15	//	600	400 g	67%	5 mm

[1] Wet- milled sample.

The samples were then sieved down to reduce the particle size below 45 µm with a 3-step series of sieves of 150 µm, 100 µm and 45 µm. Both the ball mill and the sieve stack were produced by Retsch, the former being the PM100 Planetary ball mill.

2.1 More on the milling parameters

The 20 hours milling time was based on other studies employing milling as mechanical alloying process [5][6]. In order to explore the possibility of reaching a balance between cold welding and fracturing of the powders [7], one sample was milled for 40 hours.

The milling time was divided in 10 minutes of milling and 15 minutes of cooling down, after which the direction of milling is reversed. This was done to prevent overheating of the grinding jar and to maximize the effectiveness of the Process Control Agents (PCAs), which tend to evaporate quickly if high temperatures are reached, which nullifies their effects in later stages of the milling [8].

A Process Control Agent is added in order to prevent excessive cold welding in almost all of the prepared samples. The PCA acts as a surfactant and prevent interaction between the particles. Two different PCAs (acetic acid and ethanol) are used in this study to determine whether there is a difference in their effects and which one is bestsuited for this process. In one case, no PCA is used, which provides a reference for the possible improvement of powder characteristics. The use of PCAs is wide-spread in ball milling applications and their effects are well documented [7][8][9].

The rotations per minute (RPM) of the planetary disc of the planetary ball mill were set to 600 rpm to provide high energy to the balls and to effectively grind the powder to a small size in the set time. It must be noted that the ball mill is set so that there is a 2:1 proportion between grinding jar rotations and planetary disc rotations, hence 600 rpm actually translates to 1200 rpm for the grinding jar. Sample WE-0855 was milled at 550 (1100) rpm

to reduce the machine's intense vibrations, which where caused by a slightly unbalanced counterweight system, which could not compensate up to the high mass of the grinding jar and its contents.

In order to explore the effects of a slower rotation speed on the powder, sample PA-2045 was milled at 450 (900) rpm. The high contamination of this sample requires further studies of the phenomenology of ball milling at different speeds. One hypothesis is that the impacts of the grinding balls on the grinding jar may have been the cause. The impacts may have increased greatly if the rotational speed used is below the critical speed of the system formed by the jar and the balls. The critical speed represents the threshold after which the grinding balls do not manage to detach from the walls and impact the jar and the powder and instead stay pinned on the side, reducing the impact energy transferred to the particles greatly [10].

To explore the conditions that lead to this phenomenon, a power study with the same conditions as the grinding conditions has been performed on the planetary ball mill: the rotational speed is increased in finite steps over the full range allowed by the machine and the power level is recorded and plotted. This can be seen in figure 1. A decrease in power is expected at the point where the critical speed is surpassed, due to a decrease in the work necessary to maintain the rotation once the grinding balls stop dissipating the systems energy into impact force.

There is a dip in power in the plot at 575 rpm. If this is an indication of the passing of the critical speed threshold, then it can be that during the grinding of this sample, milled with a speed below the threshold, a high amount of impact energy was transferred by the grinding balls to the powder and the grinding jar. This may have enhanced the erosion of the surface layer of the inner wall and it may have produced the high amount of contamination of the sample.
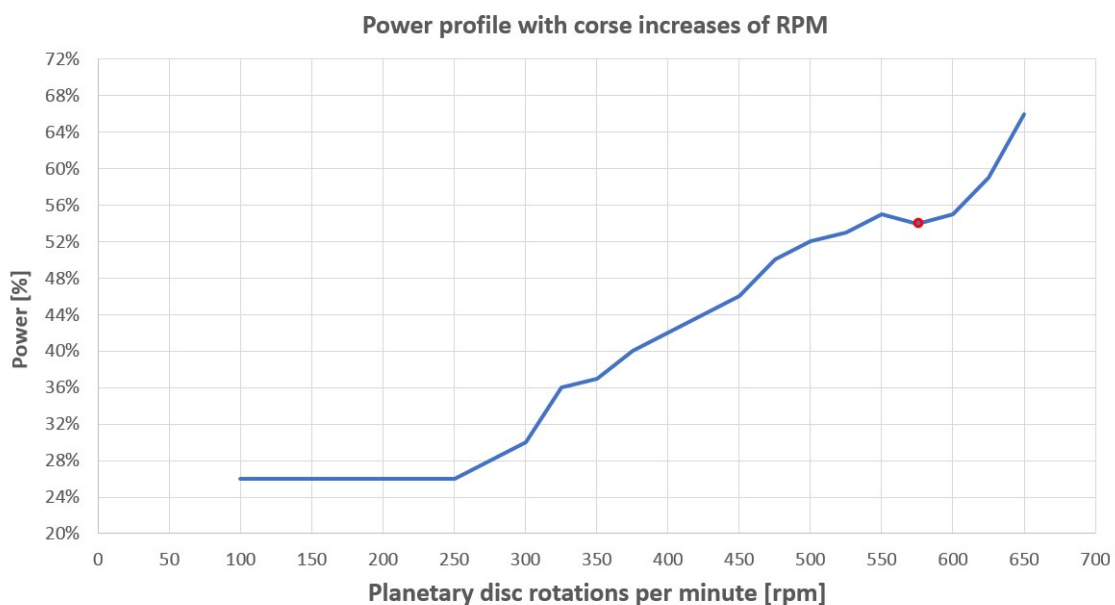

Figure 1:   Power profile of the PM100 planetary ball mill with coarse-stepped increases in rotational speed. The dip in power is highlighted in red.

The fill level of the jar and the ball size where chosen according to the guidelines provided in the Retsch PM100 Planetary ball mill manual. The mass of the powder corresponds to lowest powder volume recommended by the manual for the 250 ml grinding jar.

3 Characterization of samples

Four methods of characterization were employed to analyze the samples:

- Optical microscopy;

- Angle of repose measurement of the most promising samples;

- Electron microscope in Scanning Electron Microscopy (SEM) mode;

- Energy Dispersive X-ray spectroscopy (EDX).

3.1 Optical microscopy

The aim of this was to obtain pictures of a single layer of particles, so that it would be possible to use a specialized software to perform an automated particle size analysis. The image analysis software "ImageJ" was used for this purpose. An example of this process is shown in figures 2, 3 and 4.
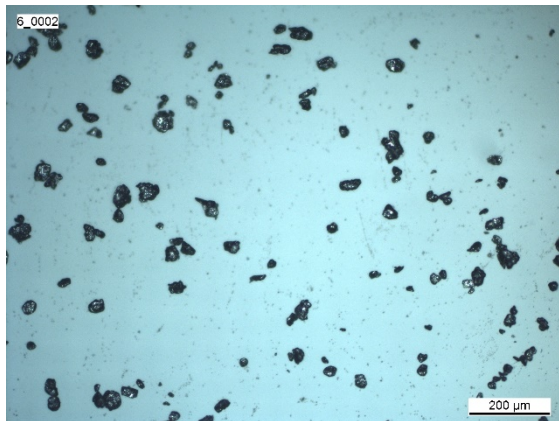

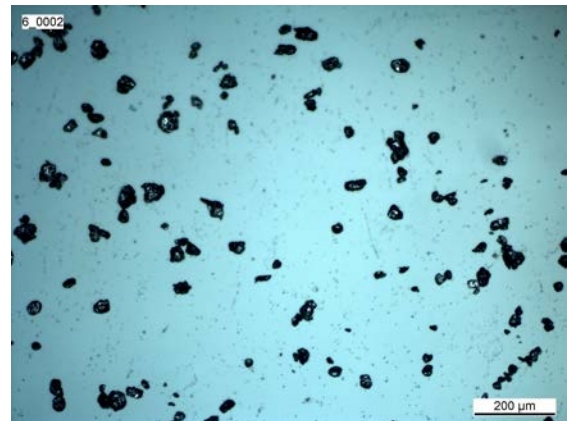*Figure 2: Unaltered optical microscopy picture of sample 6.*

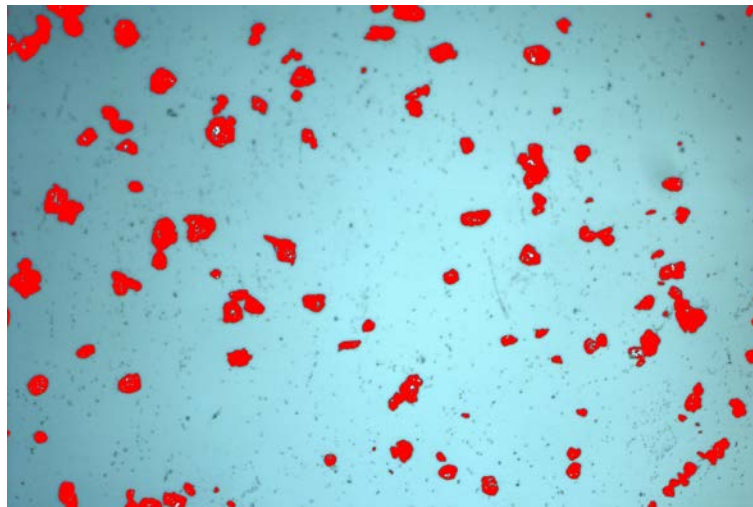*Figure 3: Brightness and contrast-adjusted picture of sample 6.*

Figure 4:   Fully processed picture of sample 6; the red areas that define the analyzed particles are clearly visible.

In all of these pictures, it is possible to see some background artifacts, which influence the results of the particle analysis by being erroneously included. To reduce this, the brightness and the contrast of this image are calibrated to define a clear difference between particles and artifacts. Afterwards, an appropriate color threshold is also selected to perform the particle analysis, which results in figure 4.

The size of the particles has been evaluated in terms of the Feret diameter, with a focus also on the minimum one measured for each particle by ImageJ. Another issue arises from the fact that some of the highlighted particles are overlapping in the picture, leading to what is perceived by the software as bigger particles. Because of the specific mesh sizes of the sieve stacks used, it is not possible that any particle with a minimum Feret diameter greater than 45 µm may have passed, hence these particles were excluded from the calculation of the avereage particle size.

The average Feret diameter is calculated as the average of the Feret diameters of all of the analyzed particle. This however, besides being strongly affected by the artifacts in the image, is also not representative of the mass distribution in the sample, as most of the mass is concentrated in the bigger particles. In order for this to be reflected in the analysis, a weighted average is performed and the chosen weight parameter is the cube of the Feret diameter itself, as an approximation of the particles' volume. Although the particles are not cubical, the cube of the Feret diameter is still the measured quantity that has the strongest connection with the volume, hence the mass, granting constant density, and therefore the best suited to be the weight in the average.

3.2 Angle of repose

The angle of repose is a measure which can be used to evaluate the flowability of the powders and hence their suitability for use in the additive manufacturing process. It represents the steepest angle that can form between the side of a pile and the horizontal plane when a powder is poured on a surface; if more powder is poured on top of the pile after the critical angle has been reached, it will simply slide to the side. An example is shown in figure 5 [11].
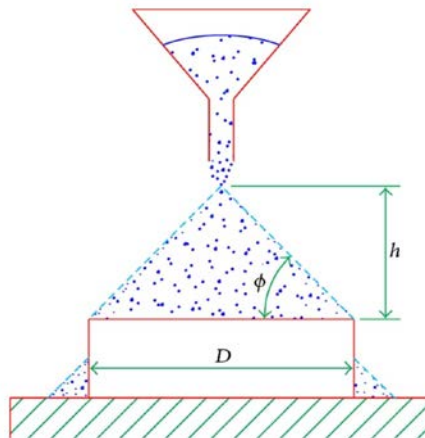
Figure 5: Measurement example of the angle of repose, indicated by φ in the figure.

The measurement was performed in a similar manner as shown in the figure, with a funnel pouring the powder on the upper circular base of a cylindrical object. However, the powder was supplied to the funnel in very small bursts, which flattened the tip of the conical pile. This made the assessment of the magnitude of the angle based on the diameter of the base and the height of the pile very inaccurate, but it was still possible to measure the inclination of the slope drectly. This was done after verifying that additional powder would not increase it but simply slide down, which signifies that the critical angle has been reached. A picture of one of the powder analyzed with this method can be seen in figure 6.

Figure 6: Example of the angle of repose measurement for sample 1.

An alternative method employed is to pour the powder on a flat surface with no boundaries and to collect multiple measurements of the angle over a long pouring session, after which an average of all of the measurements is performed.

3.3 Scanning electron microscopy

A scanning electron microscope (SEM) was employed to observe the size and shape of the grains of the ODS powders produced, as well to observe the surface features. The working principle is based on an electron beam being accelerated and focused on a minuscule point on the sample and then scanning completely its surface. The beam electrons induce the release of secondary electrons from the surface of the sample; these are collected by a detector which generates a signal that can be used to precisely reconstruct the topography

of the surface of the sample. It is possible to obtain a resolution in the nm range with this technique, but by using this only, no information is gathered on the composition of the sample.

Secondary electrons are not the only type of particles or radiation that is emitted for the samples, for example back-scattered electrons and induced x-rays can also be detected to obtain additional information.

The intended purpose of the image is obtain detailed information about the size, shape and surface morphology of the particles, and if possible to use it in an automated particle size analysis, but issues of overlapping particles made this very unreliable. A sample picture of one of the analyzed samples can be seen in figure 7.
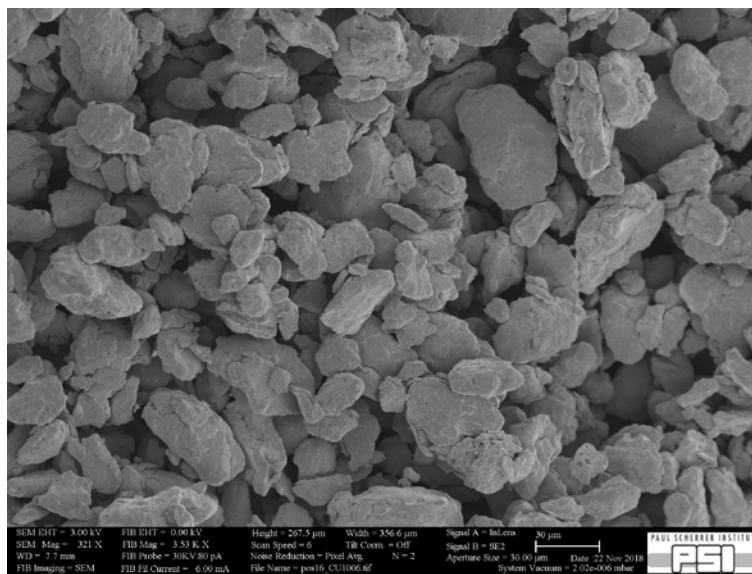

Figure 7: Picture of sample 6 taken with the SEM.

3.4 Energy dispersive x-ray spectroscopy

Different elements have very specific structures for the energy levels of the surrounding electrons. This makes it so that by analyzing the X-rays emitted during the transition of outer shell electrons to inner shell vacancies, it is possible to recognize different atoms. Energy dispersive x-ray spectroscopy (EDX) exploits this principle by exciting the electrons of the atoms of a sample, which leads to inner vacancies forming and the electron transitions that produce characteristic X-rays. These photons are detected and their energy is measured and compared with the available characteristic X-rays libraries in order to define the composition of the material. Coupled with scanning electron microscopy, it may be used to also provide information about the distribution of different elements in the material.

In this study, EDX has been used to obtain information onthe composition of the sample and to check for possible contamination and impurities. As an example, the analysis of the composition of one particle is shown in figure 8.
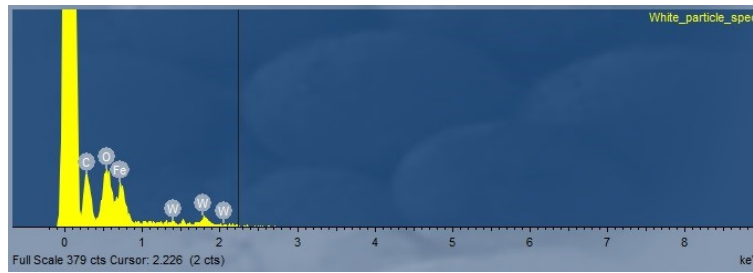
Figure 8: Analysis of a powder particle via EDX.

4 Results

The aim of the study is to identify a powder that is suitable to be used in additive manufacturing. This is evaluated mainly in terms of flowability with the angle of repose and of size with the Feret diameter. As mentioned, the flowability of the powder is of high importance to guarantee smooth operation in an additive manufacturing process. The size of the particles is also instrumental for the quality and reproducibility of the print, as small particles with narrow size distribution can be heated up and melted homogenously, which reduces the possibility of fabrication defects [12].

The full results are shown in table 3.

Table 3: Final characteristics of the milled powders.

ID	Feret [µm][1]	Weighed Feret [µm]	Angle of repose [°]
PA-2060	14.506 ± 8.529	57.730	49.883
PA-4060	11.794 ± 6.622	53.736	NA
WE-0855	NA	NA	NA
PE-2060	6.527 ± 3.820	39.243	NA
PA-2045	NA	NA	NA
D-2060	17.439 ± 10.255	60.584	36.94
D-4060	10.220 ± 5.507	39.189	40.67

[1]1-σ error bar of the set of measurements.

As can be seen from the table, not all measurements were performed for each powder sample. Samples PA-4060 and PE-2060 were excluded from the angle of repose measurement because the strong cohesive forces betwen the particles hindered the measurement. Samples WE-0855 and PA-2045 were excluded from all analyses, the former because its retrieval after the milling was deemed unfeasible and the latter due to the heavy contamination. The specific features of the different samples will be discussed separately,

but overall the process shows good control of the size of the particles is achieved but the sphericity of the particle is generally poor and the flowability becomes progressively worse as the size decreases. All of the powders have also shown a tendency to stick to the walls of the grinding jar, making collection troublesome in several cases.

4.1   Sample PA-2060

Below are several figures showing the characteristics of this sample.

Figure 9:   Optical microscopy image of image of sample PA-2060.

Figure 10: Scanning electron microscopy sample PA-2060

Figure 11: Angle of repose measurement for sample 1.

Sample PA-2060 has been milled for 20 hours with acetic acid as a process control agent. The size of the particles is appropriate for additive manufacturing, but the flowability of the powder is very poor, as shown by the angle of repose. Furthermore, the particles appear to have a very flat shape, very far from the sought sphericity, which provides a possible cause for the poor flowability.

Figure 12: Particle size distribution of sample PA-2060.

4.2 Sample PA-4060

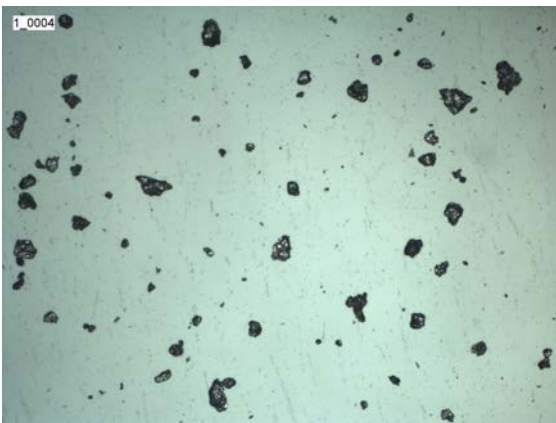Below are several figures showing the characteristics of this sample.

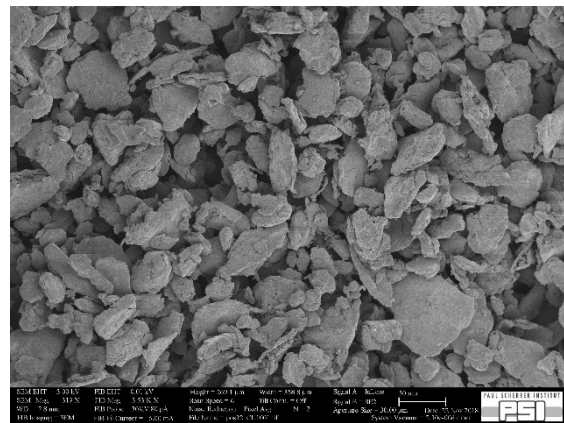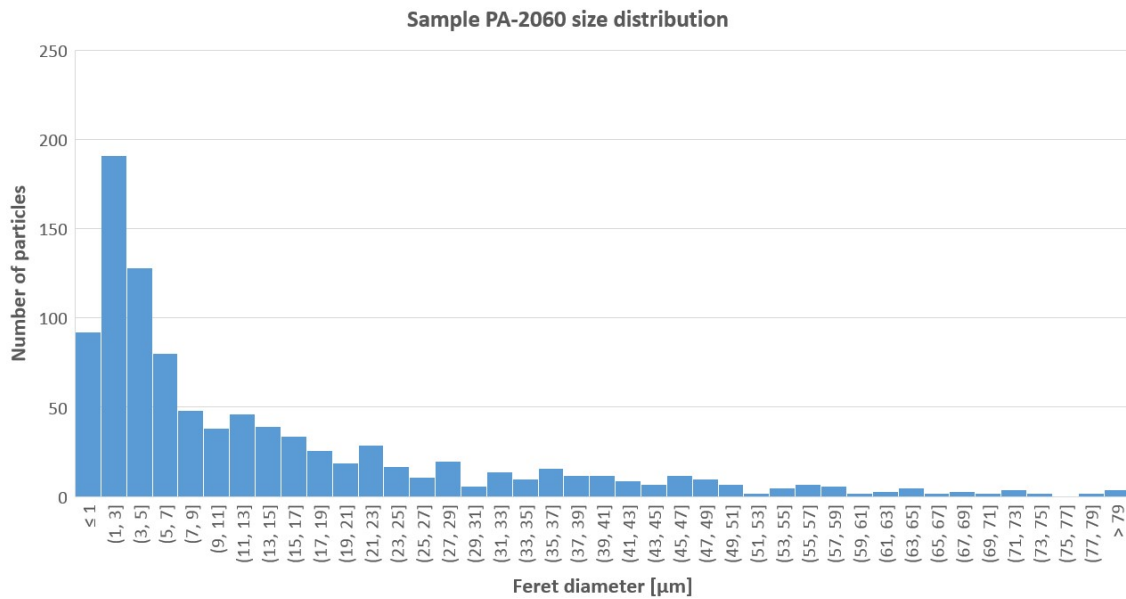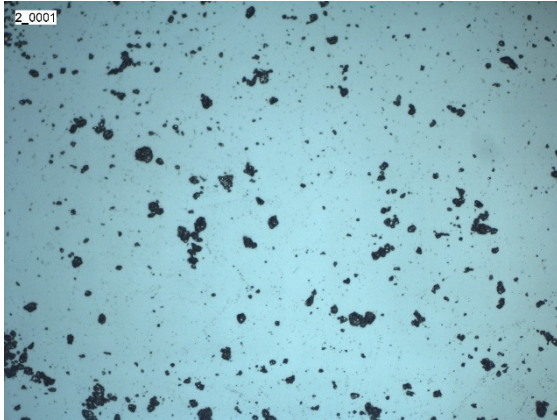*Figure 13: Optical microscopy image of image of sample PA-4060.*
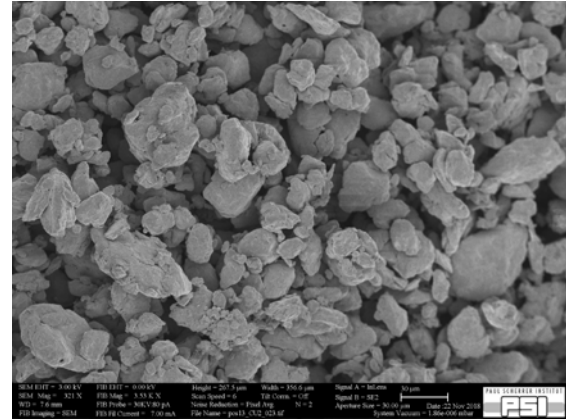
Figure 14: Scanning electron microscopy sample PA-4060.

Sample PA-4060 has been milled for 40 hours with acetic acid as a process control agent. The size of the particles is considerably lower than that from sample PA-2060, but this does not reflect well in the analysis because stacking particles below the filtering limit can alter the results to an extent. However, the deciding factor that makes this powder unsuitable for use in an additive manufacturing process is the very poor flowability. In figure 15 it is possible to see that it was not possible to create a pile suitable for the angle of repose measurement, as it is more dome-shaped than cone shaped. It is actually possible to see on the right side, by the base of the pile, an extremely steep angle, which, coupled with the very coarse profile of the pile, represents strong evidence for the powder's tendency to agglomerate and against

its flowability. For this reason, the powder is deemed incompatible with the needs of additive manufacturing.
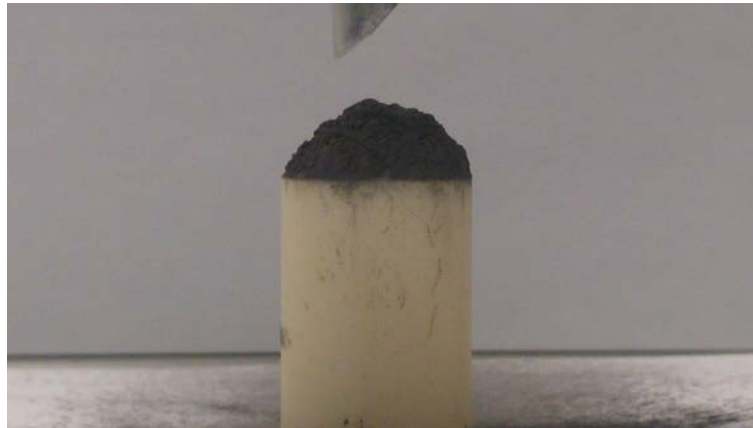
Figure 15: Angle of repose measurement for sample 2.
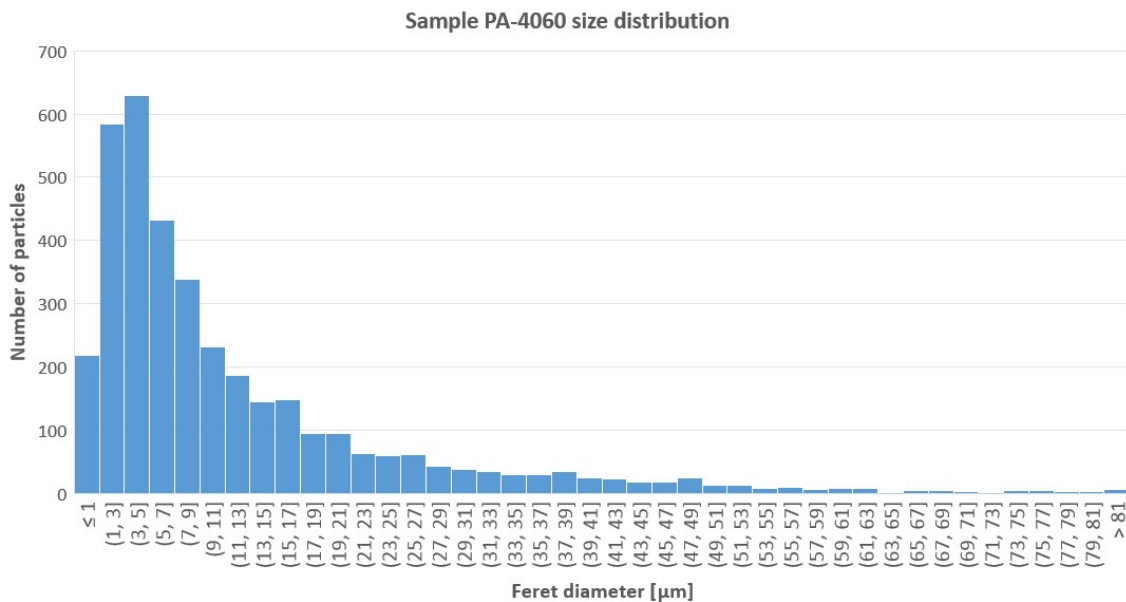
Figure 16: Particle size distribution of sample PA-4060.

4.3 Sample WE-0855

Below is a figure showing the appearance of this sample as seen with SEM.

Figure 17: SEM image of sample WE-0855.

Sample WE-0855 has been wet-milled for 8 hours in an ethanol bath. Unfortunately, the resulting mixture was not fit to be sieved without more specialized equipment, partly because the final texture and consistency were different from the desired outcome. Still it is possible to comment on the SEM analysis of the sample. The particles appear to be slightly smaller than those of sample PA-4060. The shape is not significantly different from sample PA-4060 as well, which is an improvement on sample PA-2060, but still far from the optimal spherical shape.

4.4 Sample PE-2060

Figure 18: Optical microscopy image of image of sample PE-2060.

Figure 19: Scanning electron microscopy sample PE-2060.

Below are several figures showing the characteristics of this sample. Sample PE-2060 has been milled for 20 hours using Ethanol as PCA. This sample presents the smallest particles overall but also the highest tendency for agglomeration. The latter of these characteristics makes this powder ill-suited for additive manufacturing. In particular, the tendency towards agglomeration makes it very troublesome to collect this powder, as it tends to stick to the wall of the grinding jar very strongly and it passes with difficulty through the sieve, despite the small size of the particles.

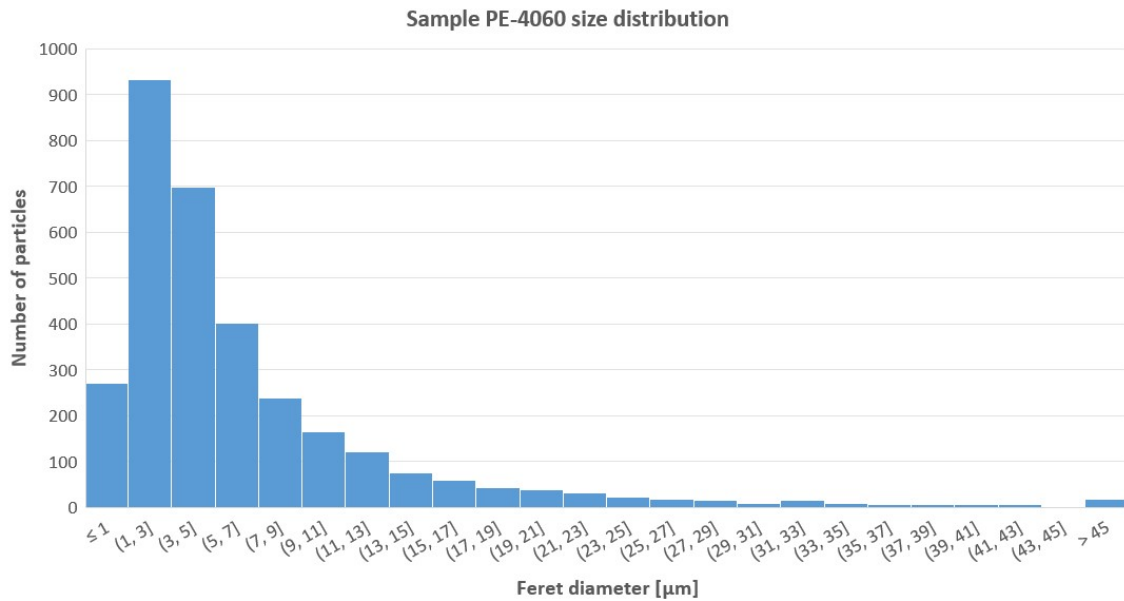*Figure 20: Particle size distribution of sample PE-2060.*

4.5 Sample PA-2045

This sample was produced to explore the effects of a slower rotation speed on the properties of the powder, hence it was milled for 20 hours with acetic acid as a process control agent at a speed of 450 rpm. However, the resulting powder was contaminated heavily during the process from an unidentified source.

The amount of powder retrieved was considerably higher than the amount placed into the grinding jar. The most likely explanations involve the detachment of material cold-welded onto the walls by previous millings or erosion of the inner wall itself; it cannot be excluded as well that the balls themselves may have been ground to powder or that the jar lid may have been eroded.

This interesting phenomenon should be further studied; the sample, however, is not evaluated in terms of compatibility with additive manufacturing, due to the large contamination and showing of high electrostatic charging.

4.6 Sample D-2060

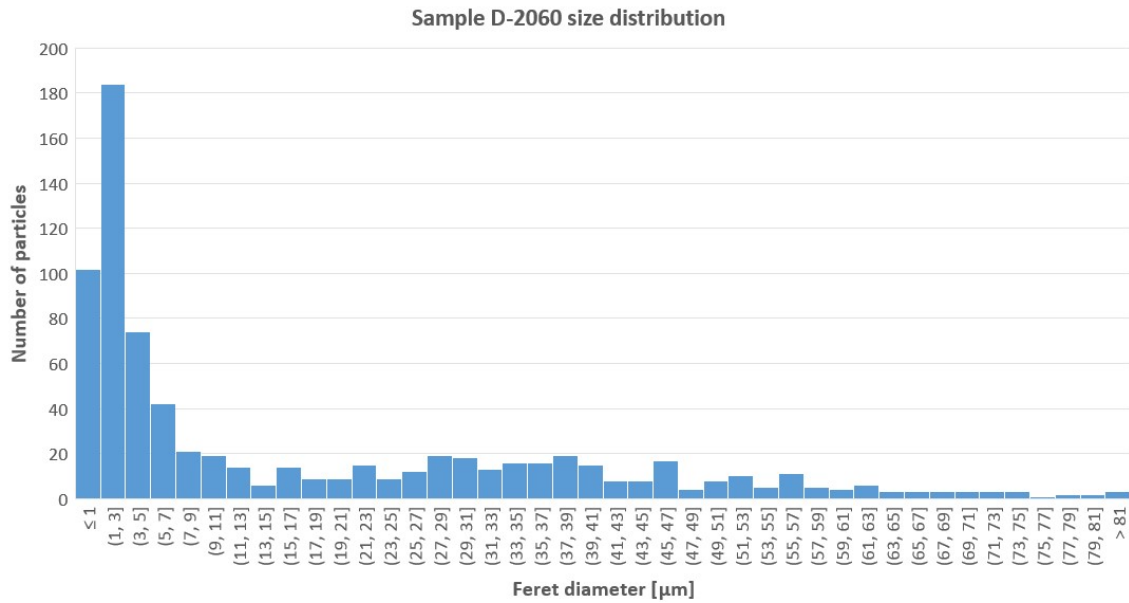Below are several figures showing the characteristics of this sample.

Figure 21: Optical microscopy image of image of sample D-2060.

Figure 22: Scanning electron microscopy sample D-2060.

Figure 23: Angle of repose measurement example for sample 6.

Sample D-2060 has been dry milled for 20 hours with no process control agent. The size of the particles is the highest, but still in an appropriate range and the angle of repose shows that the flowability is considerably better than that of the other samples. The tendency to stick on the walls of the sample is also the lowest found so far.

For these reasons, this sample is promising one in terms of additive manufacturing compatibility.

Figure 24: Particle size distribution of sample D-2060.
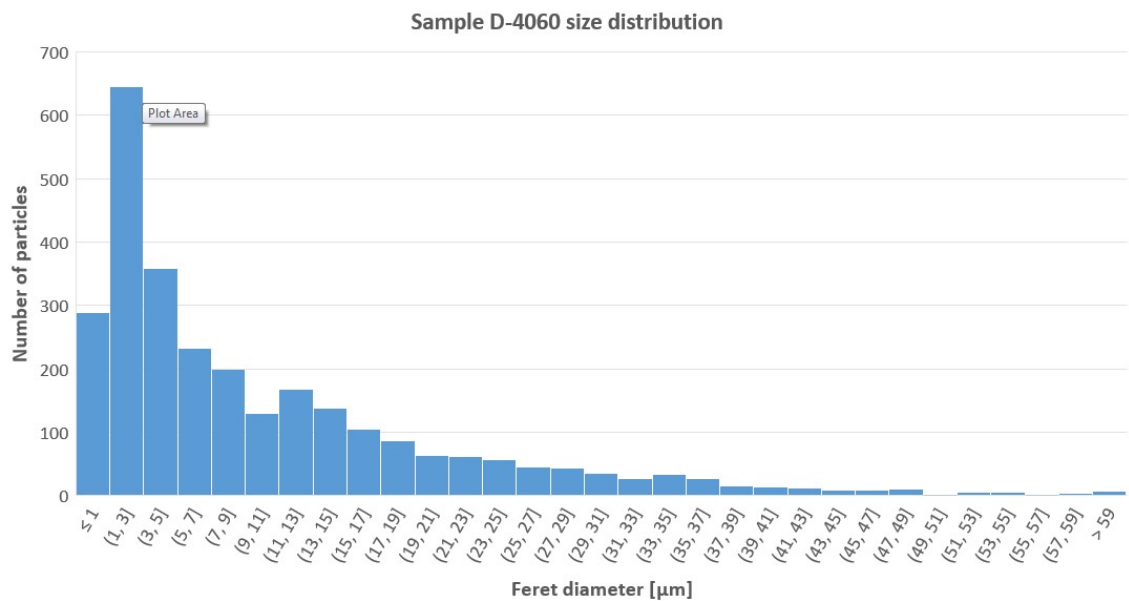
4.7 Sample D-4060

Figure 25: Particle size distribution of sample D-4060.

An additional batch has been prepared based on sample D-2060 with the objective to improve upon it and to produce an amount that would allow for the printing of the specimen. Sample D-4060 was milled for 40 hours collectively at the same rotational speed and with no PCA, in order to try to reduce the particle size and to see the impact on the flowability. Below are several figures showing the characteristics of this sample.
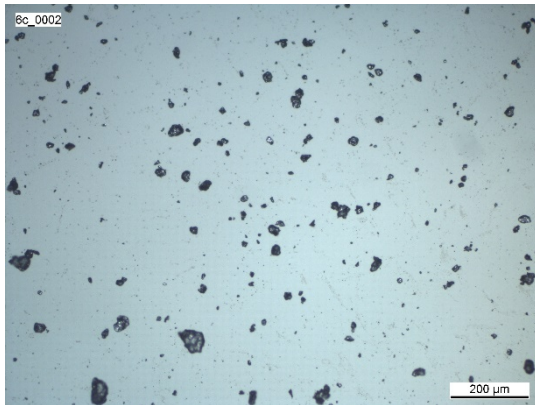
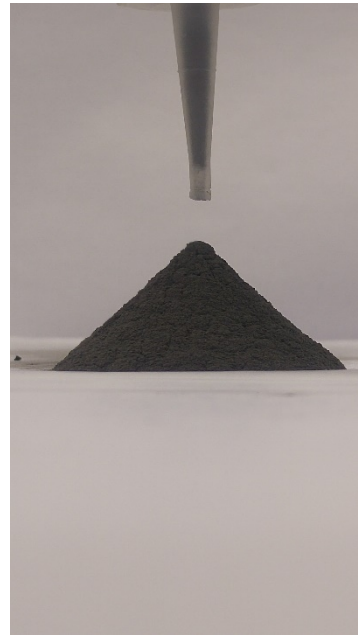*Figure 26: Optical microscopy image of sample D4060.*

Figure 27: Angle of repose measurement example for sample D4060.

As it can be seen, the particle size is substantially reduced compared to sample D2060, but the flowability has also worsened. This sample is chosen as optimal for the purpose of additive manufacturing, presenting decent, although not perfect, levels of flowability and a particle size distribution that enables a quality print to be produced.

5 Conclusions and further plans

The objective of the study was to investigate the influence of processing conditions on the size and flowability of the powder with the intent of producing one which could be used in an additive manufacturing process. Out of the produced powders, a good candidate appeared to be sample D-2060, milled with no PCA for 20 hours, because of its relatively good flowability. The usage of PCAs has been shown to reduce the size of the particles, a result that can also be obtained by increasing the milling time, but it does not by itself improve the flowability of the powder or the particle's sphericity. Based on the comparatively good properites of sample D-2060, sample D-4060 has been made, which shows a finer particle size, obtained at the cost of a worse flowability. This however is considered a good compromise of properties..

It is possible that by reducing the rotational speed of the planetary disc, the particles may retain their spherical shape [5] and a substantial improvement in terms of flowability may be found. In order to better refine the particle size distribution, further sieving steps could be employed; this could also allow a specific size range to be selected by sieving away the particles smaller than the sieve's mesh-size. These are aspects of the process that should be explored further.

Future developments of this project will include the use of the powder in the additive manufacturing process, mechanical testing of the produced ODS steel specimens, studies of the effects of additives on the formation of oxide particles and analysis of these with the use of photons from the Swiss Light Source (SLS).

Remark

This study was performed in the context of a Semester Project in the Nuclear Engineering joint MSc program of ETHZ and EPFL, between the 8th of October, 2018, and the 18th of January, 2019.

The work took place at Paul Scherrer Institute (PSI) under the supervision of Dr. P. Warnicke, P.D. Dr. M. A. Pouchon and was approved by Prof. Dr. H. M. Prasser.

References

[1]   Shigeharu Ukai and Masayuki Fujiwara. "Perspective of ODS alloys application in nuclear environments". In: *Journal of Nuclear Materials* 307-311 (2002), pp. 749–757. issn: 0022-3115.

      doi: https://doi.org/10.1016/S0022-3115(02)01043-7.

      url: http://www.sciencedirect.com/science/article/pii/S0022311502010437.

[2]   Helong Hu et al. "Fabrication and mechanical properties of a 14Cr-ODS steel". In: *Journal of Physics Conference Series* 419 (Mar. 2013), pp. 2029–.

      doi: 10.1088/ 1742-6596/419/1/012029.

[3]   Markus B. Wilms et al. "Laser additive manufacturing of oxide dispersion strengthened steels using laser-generated nanoparticle-metal composite powders". In: *Procedia CIRP* 74 (2018). 10th CIRP Conference on Photonic Technologies [LANE 2018], pp. 196–200. issn: 2212-8271.

      doi: https://doi.org/10.1016/j.procir. 2018.08.093.

      url: http://www.sciencedirect.com/science/article/pii/ S2212827118308795.

[4]   Thomas Duda and L. Venkat Raghavan. "3D Metal Printing Technology". In: *IFAC-PapersOnLine* 49.29 (2016). 17th IFAC Conference on International Stability, Technology and Culture TECIS 2016, pp. 103–110. issn: 2405-8963.

      doi: https://doi.org/10.1016/j.ifacol.2016.11.111.

      url: http://www.sciencedirect.com/science/article/pii/S2405896316325496.

[5]   Haijian Xu et al. "Microstructural evolution in a new Fe based ODS alloy processed by mechanical alloying". In: *Nuclear Materials and Energy* 7 (2016), pp. 1–4. issn: 2352-1791.

      doi: https://doi.org/10.1016/j.nme.2016.04.006.

      url: http: //www.sciencedirect.com/science/article/pii/S2352179116300011.

Semester project – A. Cavaliere
NOT CLASSIFIED

[6] Jung-Ho Ahn et al. "Preparation of nano-sized ODS alloys by ball-milling using metallic salts". In: *Journal of Alloys and Compounds* 483.1 (2009). 14th International Symposium on Metastable and Nano-Materials (ISMANAM-2007), pp. 247–251. issn: 0925-8388.

doi: https://doi.org/10.1016/j.jallcom.2008.08.138.

url: http://www.sciencedirect.com/science/article/pii/S0925838808018793.

[7] Quanquan Han, Rossi Setchi, and Sam L. Evans. "Characterisation and milling time optimisation of nanocrystalline aluminium powder for selective laser melting". In: *The International Journal of Advanced Manufacturing Technology* 88 (May 2016). doi: 10.1007/s00170-016-8866-z.

[8] Quanquan Han, Rossitza Setchi, and Sam L. Evans. "Synthesis and characterisation of advanced ball-milled Al-Al2O3 nanocomposites for selective laser melting". In: *Powder Technology* 297 (2016), pp. 183–192. issn: 0032-5910.

doi: https://doi.org/10.1016/j.powtec.2016.04.015.

url: http://www.sciencedirect.com/science/article/pii/S0032591016301747.

[9] C. Suryanarayana. *Mechanical alloying and milling.* Vol. 46. 1. 2001, pp. 1–184.

doi: https://doi.org/10.1016/S0079-6425(99)00010-9.

url: http://www.sciencedirect.com/science/article/pii/S0079642599000109.

[10] Hiroshi Mio et al. "Optimum revolution and rotational directions and their speeds in planetary ball milling". In: *International Journal of Mineral Processing* 74 (2004). Special Issue Supplement Comminution 2002, S85–S92. issn: 0301-7516.

doi: https://doi.org/10.1016/j.minpro.2004.07.002

url: http://www.sciencedirect.com/science/article/pii/S0301751604000274.

[11] Milene Minniti de Campos and Maria Ferreira. "A Comparative Analysis of the Flow Properties between Two Alumina-Based Dry Powders". In: *Advances in Materials Science and Engineering* 2013 (Dec. 2013), pp. 1–7.

doi: 10.1155/2013/519846.

[12] S. Sun, M. Brandt, and M. Easton. "2 - Powder bed fusion processes: An overview". In: *Laser Additive Manufacturing.* Ed. by Milan Brandt. Woodhead Publishing Series in Electronic and Optical Materials. Woodhead Publishing, 2017, pp. 55–77. isbn: 978-0-08-100433-3.

doi: https://doi.org/10.1016/B978-0-08100433-3.00002-6.

url: http://www.sciencedirect.com/science/article/pii/B9780081004333000026.